Makara Journal of Science 16/1 (2012) 27-32

Earthquakes Sources Parameter Estimation of 20080917 and 20081114 Near Semangko Fault, Sumatra Using Three Components of Local Waveform Recorded by IA Network Station

Bagus Jaya Santosa[1*)] and Madlazim[2]

1. Department of Physics, FMIPA, Institut Teknologi Sepuluh November, Surabaya 60111, Indonesia
2. Department of Physics, FMIPA, Universitas Negeri Surabaya, Surabaya 60231, Indonesia

[*)]*E-mail: bjs@physics.its.ac.id*

Abstract

The 17/09/2008 22:04:80 UTC and 14/11/2008 00:27:31.70 earthquakes near Semangko fault were analyzed to identify the fault planes. The two events were relocated to assess physical insight against the hypocenter uncertainty. The data used to determine source parameters of both earthquakes was three components of local waveform recorded by Geofon broadband IA network stations, (MDSI, LWLI, BLSI and RBSI) for the event of 17/09/2008 and (MDSI, LWLI, BLSI and KSI) for the event of 14/11/2008. Distance from the epicenter to all station was less than 5°. Moment tensor solution of two events was simultaneously analyzed by determination of the centroid position. Simultaneous analysis covered hypocenter position, centroid position and nodal planes of two events indicated Semangko fault planes. Considering that the Semangko fault zone is a high seismicity area, the identification of the seismic fault is important for the seismic hazard investigation in the region.

Abstrak

Estimasi Parameter Sumber Gempa Bumi 20080917 dan 20081114 di Dekat Zona Sesar Semangko dengan Menggunakan Rekaman Lokal Waveform Tiga Komponen oleh Jaringan Stasiun IA. Gempa bumi yang terjadi pada 17/09/2008 22:04:80 dan 14/11/2008 00:27:31.70 UTC dekat Semangko dianalisis untuk identifikasi bidang patahannya. Kedua gempa bumi tersebut direlokasi untuk menilai pandangan fisis terhadap ketidakpastian hiposenter. Data yang digunakan untuk menentukan parameter gempa kedua sumber adalah seismogram penuh tiga komponen lokal direkam oleh Geofon IA broadband stasiun jaringan (MDSI, LWLI, BLSI dan RBSI) untuk gempa pada 17/09/2008 dan untuk gempa pada tanggal 14 /11/2008 oleh stasiun jaringan (MDSI, LWLI, BLSI dan KSI). Jarak dari semua stasiun menuju pusat gempa kurang dari 5°. Solusi momen tensor dari kedua gempa dianalisis bersamaan dengan penentuan posisi pusat gaya (centroid)-nya. Analisis simultan meliputi posisi hiposenter, posisi centroid dan bidang nodal dari gempa menunjukkan bidang patahan Semangko. Arah strike dari dua gempa ini sesuai dengan arah Zona Sesar Sumatera. Menimbang bahwa zona sesar Semangko merupakan daerah rawan gempa, identifikasi atas bidang patahan seismik ini penting untuk meneliti bahaya seismik daerah tersebut.

Keywords: earthquake source, Semangko fault planes, waveform inversion

1. Introduction

Magnitude values of two earthquakes on 17/09/2008 at 22:04:80 UTC and 14/11/2008 at 00:27:31.70 UTC are 4.8 and 5.1 respectively. These are recorded by IA local stations and reported to Geofon which can be accessed at http://geofon.gfz-potsdam.de/geofon/new/netabs/ia_req.html. Intensity of both events is between III-IV MM. People of this area experienced a strong shocked by these two events, especially by the event of 17/09/2008, since it was taken place at Sumatra plain. Moment tensor solution of both earthquakes is not yet listed in global CMT catalogue (http://www.globalcmt.org/CMTsearch.html), Geofon (http://www.webdc.eu), BMKG (http://www.bmkg.go.id) or other seismology agencies.

SFZ (Semangko Fault Zone) accommodates most of the right-lateral strain from slab relative movement and has suggested as an active zone since Mid-Miocene [1]. West Sumatra is the border of ocean slab consists of two faulting systems, which are strike-slip faulting system that rotate toward right direction (sinitral) and interface dip-slip subduction which has bigger influence [2].

In this article, we provide three components waveform analysis of local data that was recorded by Geofon IA network, installed around Semangko fault, South Sumatra, to predict earthquake source parameters, identify the fault plane of both earthquakes, and predict its length and width and also the slip of the rupture.

The study of August 2008's earthquakes focused only on 2 events, presented in Table 1, in which the standard earth model was used as calculation of travel time. Hypocenter relocation was performed by 28 stations, as shown in Figure 1. Manual picks travel time of the P and S waves and crustal earth model used is presented in Table 2. The hypocenters were relocated and coded as HYPOINVERSE [3]. During relocation, some tests were carried out in order to use the most appropriate 1-D model and choose the parameters that will lead to the most stable results. The modified H-S model (Table 2) was applied, in which the P earth model is taken from Haslinger *et al*. [4] and the S earth model is taken form Santosa [5]. The criteria for choosing the most suitable crustal model was the RMS standard value, ERH and ERZ errors calculated using the HYPOINVERSE [3].

The errors showed that the best crustal earth model leads to the smallest error. The appropriate H-S model for the corresponding research location is listed in Table 2.

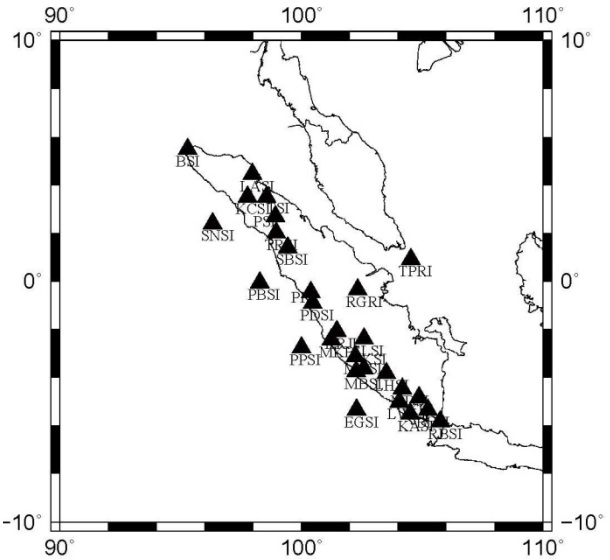

Figure 1. The Stations of IA Network in Sumatra

Table 1. Two Events Announced by Geofon

Date	Time (UTC)	Latitude (degree)	Latitude (degree)	Depth (km)	Mw
2008/09/17	22:04:49.8	-4.72	104.34	177	4.7
2008/11/14	00:27:37.1	-6.09	105.41	146	5.1

Table 2. H-S velocity Model Modified for the Location

V_p (km/s)	Depth (km)
2.31	0.0
5.52	2.1
6.23	5.0
6.41	16.0
6.70	33.0

2. Methods

The waveform was processed using the Seismic Analysis Code (SAC) software, the instrumental correction was first performed on the selected seismogram [6], the corrected seismograms were then integrated to compute the velocity traces. However, the instrumental corrections on the broadband seismograms were applied using built in facility of the ISOLA (Isolated Asperity) software. The corrected velocity traces were cut from origin time to 250 s and subjected to filter between 0.01 and 5.0 Hz using 4 pole band-pass Butterworth filter facility which provided in SAC. The input of ISOLA code is the band-pass filtered velocity seismogram records, which then integrated to generate band-passed seismogram displacement available in ISOLA. Finally, these displacement traces were used as data input for the full waveform moment tensor inversion, available in the ISOLA software.

Green function was calculated using discrete wave number method [7]. To calculate Green function for waveform modeling, we used 1-D velocity model shown in Table 3, since all elastic parameters for Green function calculation are required.

The three components waveform inversion was conducted using iterative deconvolution method [8-9], where the stop criteria is the waveform fitting, which is shown by the variance reduction values. This method was implemented in ISOLA software [10] as a numerical simulation program development [11-12], to obtain earthquake source parameters. After the earthquake's source parameters obtained, they were used to determine the orientation fault planes (main and auxiliary normal planes), length and width and also slip length of both earthquakes. To determine the valid fault plane orientation (one of these planes), H(ypocenter)-C(entroid)-plot method was used [13]. While in

Table 3. H-S Velocity Model Modified for Full Waveform Inversion

V_p(km/s)	V_s(km/s)	ρ (g/cm^3)	Q_p	Q_s
2.31	1.30	2.50	300	150
2.31	2.40	2.90	300	150
5.52	3.10	3.00	300	150
6.23	3.50	3.30	300	150
6.41	3.60	3.40	300	150
6.70	4.70	3.40	300	150
8.00	4.76	3.50	1000	500

Table 4. Two Events as Located in this Article by HYPOINVERS and from GEOFON

Date	Origin	HYPOINVERS								GEOFON		
		Latitude (degrees)	Longitude (degrees)	Depth (km)	No. P&S	RMS	ERH	ERZ	M_w	Latitude (degrees)	Longitude (degrees)	Depth (km)
2008/09/17	22:04:49.8	-4.79	104.45	176	24	0.83	2.7	1.8	4.7	-4.72	104.34	177
2008/11/14	00:27:31.7	-6.09	105.59	128	26	0.79	1.5	2.3	5.1	-6.09	105.41	146

determining the length and width of faulting plane and also slip length, an empirical equation implemented in Coulomb3.09 [14] and [15] software was used.

3. Results and Discussion

The hypocenters of the both events are presented in Table 4 by the authors. RMS value of these two events shows as small as <0.9, which is difficult to achieve. It also depends on the earth model applied. We use Geofon's hypocenter as the initial position of the earthquake source, iteration gives a smaller RMS value and it is stopped when the change of RMS value is smaller than suggested parameter. Depth determination results from authors differ from Geofon's. First Geofon used standard/global earth model which is not suitable for this region. Second is, because Geofon only used P travel time analysis, while the author used hypoinverse method to relocate the earthquake hypocenter and also the waveform inversion to determine the centroid point. The waveform inversion is sensitive against earth model. The obtained centroid and hypocenter points are then used to determine the valid fault plane.

Earthquake Source Parameters are used for microzonation and seismic risk treatment [14]. Seismic moment (M_0), magnitude moment (M_w), depth, fault plane orientation, length, width and slip of rupture are determined for the both events. On this analysis, the author used three components of local waveform. Earthquake source parameters can be extracted from mathematical model, if valid waveform fitting achieved between measured and synthetic seismogram. The searching process of highest DC value and its variance reduction are two important parameters to obtain the depth of earthquake source and best seismograms fitting. The best obtained Double couple (DC) value and its variance reduction for both events are 97.4% and 70% and also 87.7% and 73%, respectively (refer to Fig. 2 and 3).

The principal of HC-plot is to put hypocenters from authors (Table 3) and calculate its distance to both fault planes. In 17/09/2008 event (Fig. 3a) it was discovered that centroid hypocenter distance is 17.43 km, distance of nodal plane 1 (horizontal) to hypocenter is 16.76 km while distance of nodal plane 2 (black) to hypocenter is 3.24 km. The black nodal plane 2 is the fault plane because it is closer to the hypocenter compare to others. Therefore, the valid fault plane is nodal plane 2 (280°, 81°).

The output of HC-plot method in 14/11/2008 event (Fig. 3b) shows that distance of nodal plane 1 (vertical) to hypocenter is 3.82 km and distance of nodal plane 2 (horizontal) to hypocenter is 20.97 km. The green nodal plane 1 is the fault plane because it is closer to the hypocenter than one. Therefore, the valid fault plane is nodal plane 2 (269°, 66°). The source parameters were used to calculate length, width and slip of the rupture. Length, width and slip of rupture of event 17/09/2008 and event 14/11/2008 are 1.4 km; 1.74 km; right lateral=0.06 m and reverse slip=0.11 m and 3.29 km; 3.18 km; right lat=-0.16 m and reverse slip=-0.02 m, respectively.

On the Tables 5, the authors present the comparison of the inversion result, reviewed from DC percentage, the variance reduction for three earth crust models [4-6,16] of both events, to prove which earth model is the best for this region.

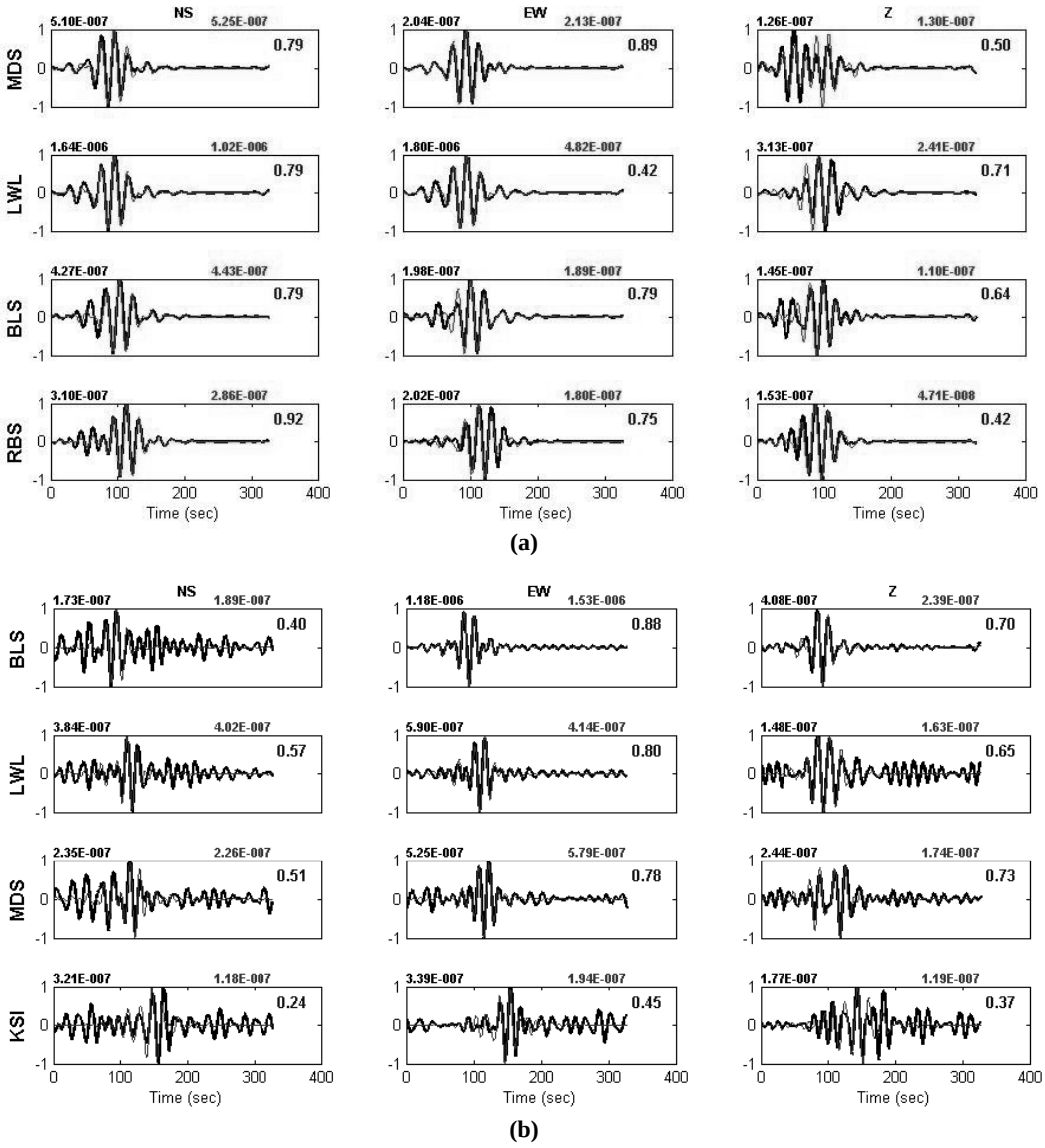

Figure 2. (a) Fault Plane Identification of 17/09/2008 Event and (b) Fault Plane Identification of 14/11/2008 Event; Observed (▪), Synthetic (▫)

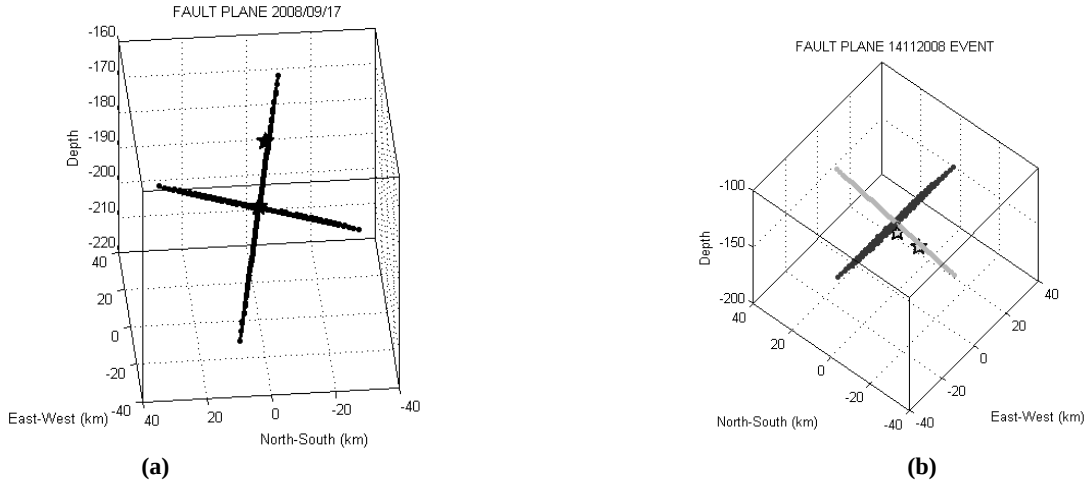

Figure 3. (a) Fault Plane Identification of 17/09/2008 Event and (b) Fault Plane Identification of 14/11/2008 Event

Table 5. DC and Variance Reduction Value Comparison for 17/09/2008 and 14/11/2008 Event

Crustal model	17/09/2008 event		14/11/2008 event	
	DC(%)	Reduction variance (%)	DC(%)	Reduction variance (%)
Haslinger *et al*. & Santosa [4-5]	97.4	70	87.7	73
Haslinger *et al*. [4]	67	47	59	39
Novotny *et al*. [16]	38	54	48	44

Table 6. Earthquake Parameters of 20080917 Event

St	Δ(km)	D (km)	M_0x10^{16} (N-m)	M_w	Stk	Dip	rak	p(km)	l(km)	rl(m)	rv_s(m)
MDS	31,488	188	0.9690	4.7	280°	81°	119°	1.40	1.74	0.06	0.11
LWL	45,326										
BLS	123.297										
RBS	199.038										

Table 7. Earthquake Parameters 20081114 Event

St	Δ (km)	D (km)	M_0x10^{16} (N-m)	M_w	Stk	Dip	rak	p (km)	l (km)	rl (m)	rv_s (m)
MDS	81.948	138	7.6836	5.1	269°	66°	-6°	3.29	3.18	-0.16	-0.02
LWL	190.989										
BLS	223.835										
KSI	412.706										

Hypocenters accuracy and focal estimation mechanism provide important information regarding the earthquake strength, orientation, length, width and slip of the rupture. The DC values of both events show that the magnitude is over 60%, means that the suggested fault planes are valid. This research criticizes research results in some articles, which is still using the teleseismic stations, polarity of Pg and Pn waves, and also moment tensor inversion, evaluated only on one component [17-40] to determine earthquake source. In this research, we used three components of local broadband, recorded by Geofon IA network stations. Station code (St), distance (Δ), centroid depth (d), M_0, M_w, strike (stk), dip, rake (rak), fault plane length (p) and width (l) and right lateral (rl) also reverse slip (rv_s) for each events are presented in Table 6 and 7.

The strike line direction of both events is pointing toward west (280° and 269°). Fault plane slope for both events are almost perpendicular to the earth surface (dip angle), which are 81° and 66°, respectively. The preferable seismotectonic interpretation is that the two events activated Semangko fault zone at a depth of about 176 km and 128 km, respectively, according to the intraplate collision.

4. Conclusions

Earthquake parameters of both events was extracted after fitting between measured and synthetic seismogram against a double couple (DC) value and variance reduction of both events achieved above 60%. Means earthquake source is a double couple fault plane. Using HC-plot method, we discovered that the valid fault plane for the both events, also to discover strike, dip and rake from its fault plane and type of the both events are reverse oblique and strike slip oblique. Length, width and slip of rupture for the both events can also be determined. The strike line direction of both events is pointing toward west (280° and 269°). The seismotectonic interpretation is that these two events activated Semangko fault zone according to the intraplate collision which conforms to the Bukit Barisan direction. The Semangko fault zone is a high risk seismicity area, the identification of the seismic fault is important for the seismic hazard investigation in the region.

Acknowledgement

We would like to express our gratitude to GFZ-Potsdam Geofon-German and BMKG-Indonesia that permitted us to download the waveform data recorded by IA network stations. Furthermore we extend our thanks to Prof. Dr. Zahradnik and Dr. Efthimios Sokos who guided us in understanding of ISOLA-GUI and HC-plot software and also apply this software to estimate earthquake source parameters using three components local waveform (http://seismo. geology.upatras.gr/isola). Thank you for Prof. Dr. Toda, Prof. Dr. Stein, Prof. Dr. Reasenberg, Prof. Dr. Dieterich, and Prof. Dr. Yoshida who give guidance in estimating the length and width of

fault plane block and also slip length using Coulomb3.109 software (http://quake.wr.usgs.gov/research/deformation/modeling/home/swf).

References

[1] D.H. Natawidjaya, Thesis, California Institute of Technology Pasadena, California, 2002.

[2] A.J. McCarthy, C.F. Elders, In: A.J. Fraser, S.J. Matthews, R.W. Murphy (Eds.), Cenozoic Deformation in Sumatra: Oblique Subduction and the Development of the Sumatran Fault System, Petroleum Geology of Southeast Asia, Special Publications, vol. 126. Geological Society, London, 1997, p.355. doi:10.1144/GSL.SP.1997.126.01.21.

[3] F.W. Klein, HYPOINVERSE, A Program for VAX and Pro-350 Computers to Solve Fore-earthquake Locations and Magnitudes, U.S. Geological Survey Open-File Report 85-515, 1985.

[4] F. Haslinger, E. Kissling, J. Ansorge, D. Hatzfeld, E. Papadimitriou, V. Karakostas, K. Makropoulos, H.-G. Kahle, Y. Peter, Tectonophysics 304 (1999) 201.

[5] B.J. Santosa, Jurnal MIPA 13 (2005) 23.

[6] A. Serpetsidaki, E. Sokos, G.-A. Tselentis, J. Zahradnik, Tectonophysics 480 (2010) 23.

[7] M. Bouchon, Bulletin of the Seismological Society of America, 71 (1981) 959.

[8] J. Zahradnik, A. Serpetsidaki, E. Sokos, G.A. Tselentis, Iterative Deconvolution of Regional Waveforms and a Double-Event Interpretation of the Lefkada Earthquake, Greece, 2006, *http://seismo.geology.upatras.gr/isola/*.

[9] M. Kikuchi, H. Kanamori, Bulletin of the Seismological Society of America, 81 (1991) 2335.

[10] E. Sokos, J. Zahradník, Computers & Geosciences 34 (2008) 967.

[11] O. Coutant, Program of Numerical Simulation AXITRA, Research Report, LGIT, Grenoble, 1989.

[12] P. Mandal, C. Satyamurty, I.P. Raju, India Tectonophysics 478 (2009) 143.

[13] J. Zahradnik, F. Gallovic, E. Sokos, A. Serpetsidaki, G.A. Tselentis, Seismol. Res. Lett. 79 (2008) 653.

[14] D.L. Wells, K.J. Coppersmith, Bull. Seismol. Soc. Amer. 84 (1994) 974.

[15] S. Toda, R.S. Stein, P.A. Reasenberg, J.H. Dieterich, A. Yoshida, J. Geophys. Res. 103 (1998) 24543.

[16] O. Novotný, J. Zahradník, G.A. Tselentis, Bull. Seismol. Soc. Amer. 91 (2001) 875.

[17] K.M. Marzooqi, A. Elenean, A.S. Megahed, I. El-Hussain, A.J. Rodgers, E. Al Khatibi, Tectonophysics 460 (2008) 237.

[18] P.K. Khan, Gondwana Research 12 (2007) 468.

[19] P. Rao, N. Kumar, P. Kalpna, T. Tsukuda, D.S. Ramesh, Gondwana Research 9 (2006) 365.

[20] D. Stich, R. Martín, J. Morales, Tectonophysics, 483 (2010) 390.

[21] J. Šílený, Tectonophysics 383 (2004) 133.

[22] J. Braunmiller, U. Kradolfer, M. Baer, D. Giardini, Tectonophysics 356 (2002) 5.

[23] K. Chang, W. Chi, Y. Gung, D. Dreger, W.H.K. Lee, C. Hung-Chie, Tectonophysics 511 (2011) 53.

[24] J. Horálek, J. Šílený, T. Fischer, Tectonophysics 356 (2002) 65.

[25] J. Sileny, R. Hofstetter, Tectonophysics 356 (2002) 157.

[26] J. Šílený, A. Milev, Tectonophysics 456 (2008) 3.

[27] A. Barth, F. Wenzel, Tectonophysics 482 (2010) 160.

[28] L. Fojtíková, V. Vavryčuk, A. Cipciar, J. Madarás, Tectonophysics 492 (2010) 213.

[29] C. Qin, C. Papazachos, E. Papadimitriou, Tectonophysics 359 (2002) 29.

[30] G. Galgana, M. Hamburger, R. McCaffrey, E. Corpuz, Q. Chen, Tectonophysics 432 (2007) 63.

[31] C. Christova, Tectonophysics 384 (2004) 175.

[32] C-P. Lee, K-H. Kim, B-S. Huang, W-G. Huang, Tectonophysics 511 (2011) 27.

[33] A. Kiratzi, Tectonophysics 490 (2010) 115.

[34] P. Mandal, S. Horton Tectonophysics 429 (2007) 61.

[35] Y.G. Wan, Z.L. Wu, G.W. Zhou, Tectonophysics 390 (2004) 235.

[36] E. Buforn, P. Coca, Tectonophysics 356 (2002) 49.

[37] A.M. Dziewonski, G. Ekström, N.N. Maternovskaya, Phys. Earth Planet. Inter. 136 (2003) 145.

[38] S.A. Sipkin, C.G. Bufe, M.D. Zirbes, Phys. Earth Planet. Inter. 130 (2002) 129.

[39] D. Dreger, B. Woods, Tectonophysics 356 (2002) 139.

[40] S. Chevrot, M. Sylvander, B. Delouis, Tectonophysics 510 (2011) 239.